

## METHOD FOR CHARACTERIZING OBSTACLES ON THE ROAD TO EVALUATE THEIR IMPACT ON POLLUTION

Manuel Infante-Francés y Tomás de J. Mateo-Sanguino

Universidad de Huelva. Avenida de las Artes, s/n - 21007 Huelva (España)

Received: 21/feb/2022 • Reviewing: 24/feb/2022 • Accepted: 27/may/2022 | DOI: <https://doi.org/10.6036/10503>

To cite this article: Infante Francés, Manuel; Infante Francés, Manuel. METHOD FOR CHARACTERIZING OBSTACLES ON THE ROAD TO EVALUATE THEIR IMPACT ON POLLUTION. DYNA. July – August 2022. vol. 97, n.4, pp. 392-397. DOI: <https://doi.org/10.6036/10503>

### ABSTRACT:

**Traffic calming measures combat speeding and other unsafe behavior by drivers, proving effectiveness in reducing the frequency and severity of accidents. However, some measures include road bumpers that cause negative impact on the environment. This work analyzes the repercussion of reducing the vehicle speed on contaminating emissions and fuel consumption (FC) when driving over a bump. To do this, this paper presents a procedure based on two methods applied to RDVs. The first, based on an application, measures the physical impact on a vehicle from acceleration taken with the IMU of a smartphone in a direction perpendicular to the chassis. The second infers the increase in emissions and FC by taking the speed-time profile of a road. The experimentation with a standard two-passenger vehicle circulating on a road with RDV of trapezoidal and circular sections vs without RDV found a significant physical impact in both scenarios, increasing the emissions of CO, HC, NO<sub>x</sub>, CO<sub>2</sub> and FC by decreasing 10 and 10 km/h. This demonstrates the generalization and usefulness of the method to study the increase in emissions and FC of «traffic calming» measures.**

**Keywords: Fuel Consumption, Pollutant Emissions, Impact, Speed Reducer, Acceleration**

### RESUMEN:

Las medidas de «traffic calming» combaten el exceso de velocidad y otras conductas inseguras de los conductores, demostrando eficacia para reducir frecuencia y gravedad de los accidentes. Sin embargo, algunas medidas incluyen resaltos en la vía que causan impacto negativo en el medio ambiente. Este trabajo analiza la repercusión que tiene aminorar la velocidad de un vehículo sobre emisiones contaminantes y consumo de combustible (FC) al aproximarse a un resalto. Para ello, este artículo presenta un procedimiento basado en dos métodos aplicados a RDVs. El primero, basado en una app, mide el impacto físico sobre un vehículo a partir de la aceleración tomada con la IMU de un smartphone en dirección perpendicular al chasis. El segundo infiere el aumento de emisiones y FC tomando el perfil de velocidad-tiempo del trayecto. La experimentación con un vehículo estándar de dos pasajeros circulando sobre un tramo con RDV de sección trapezoidal y circular frente al mismo tramo sin RDV encontró un impacto físico significativo en ambos escenarios, aumentando las emisiones de CO, HC, NO<sub>x</sub>, CO<sub>2</sub> y FC al disminuir la velocidad en 10 y 20 km/h. Ello demuestra la generalización y utilidad del método para estudiar el aumento de emisiones y FC con medidas de «traffic calming».

Palabras Clave: Consumo de Combustible, Emisiones Contaminantes, Impacto, Reductor de Velocidad, Aceleración

## FUNDING

This work has been funded by the General Secretariat for Universities, Research and Technology within the scope of the Andalusian Plan for Research, Development and Innovation (PAIDI 2020) and the European Regional Development Fund.

## 1. - INTRODUCTION

The concept of traffic calming was introduced in Delft (The Netherlands) in 1970 and spread throughout Europe, Canada, the USA and Australia. In 1997, the Institute of Transportation Engineering (ITE) developed a standard definition in response to the different interpretations of the term. Thus, traffic calming is the combination of mainly physical measures that reduce the negative effects of motor vehicle use, alter driver behavior and improve conditions for non-motorized road users [1].

Numerous studies demonstrate the effectiveness of traffic calming measures in reducing vehicle speeds and, consequently, the frequency and severity of traffic accidents [2]-[3]. Speed reduction devices (SRDs) are installed to maintain a reduced speed on certain stretches of road [4]. They are present on urban and rural roads and are often integrated in traffic calming measures, resulting in speed humps that induce the driver to reduce speed. Their effectiveness was studied in different models, concluding that their effect is restricted to a range of 20-30 m before and after them [5]. Their effectiveness lies in creating a vertical acceleration to vehicles, which transmits discomfort to their occupants when driving at speeds higher than the established speed [4]. Therefore, driving through them can reduce the feeling of comfort inside the vehicle and even cause damage due to the impact caused.

Some studies have analyzed the impact of RDVs based on acceleration measurements obtained with complex systems, accelerometers and auxiliary devices such as cameras or in-vehicle data acquisition systems [6]-[8]. The use of smartphones in scientific research, education and industrial applications is increasing, bringing innovation and enriching the environment with smart

technologies [9]. Accuracy tests of inertial sensors in smartphones reveal their reliability and high potential in intelligent transportation systems applications. In this sense, their usefulness in describing vehicle dynamics, recognizing maneuvers, and modeling fuel estimation and ecological behavior from accurate geometric road data is demonstrated [10]. Its feasibility to characterize RDVs using accelerations obtained with smartphones has also been demonstrated [11].

On this basis, this work characterizes RDVs from measurements acquired in situ with an everyday smartphone through the Sense-it app [12]. This data acquisition system has met the needs of the research using a single device, which, in addition to reducing complexity with respect to the instrumentation used in the studies consulted, is within the reach of any user. The app has allowed access to the smartphone's IMU to extract acceleration measurements in the XYZ system of the vehicle under test, record them at an appropriate sampling rate, observe them in real time on graphs, and export them to spreadsheets for further processing and analysis. Another aspect that has motivated the use of Sense-it is that, in addition to giving the user access to all the sensors on a smartphone, is integrated into the citizen science-based nQuire-it web platform [12]. Thus, the use of smartphones in research is presented as an ideal resource for raising citizen awareness and enhancing its scalability since users from anywhere can collaborate by performing supervised tasks based on data collection from their environment.

When a driver slows down before reaching a shoulder and crosses it at low speed, he avoids further physical impact. This involves decelerations and accelerations leading to increased exhaust emissions, fuel consumption (FC) [1]-[2], [13] and tire and brake particulates [14]. This driving style was analyzed against eco-driving [15]-[18]. Measurements aboard a passenger car on bumpy roads showed significant increases in CO<sub>2</sub>, CO, NO<sub>x</sub> and THC [19]. Some measures involve less severe speed reduction than usual RDVs providing pedestrian safety with less environmental impact [20]-[21]. However, the speed reduction induced by their presence is unnecessary in the absence of pedestrians on the road.

The objective of this paper is to contribute to the current state of the art in road safety by presenting a complementary approach to the issue leading to environmental benefits. Unlike the studies consulted that investigate the environmental effects of reducing speed or the physical impact of speed humps, here both aspects are evaluated jointly. To this end, this work quantitatively relates the knowledge concerning them. This perspective reveals the need to implement alternative traffic calming solutions that involve vehicle and pedestrian safety while respecting the environment.

The present method is based on two parallels: *i*) aggressive or sporty driving behavior [22] according to a speed-time profile (SVP) associated to a road with VDRs; *ii*) normal driving behavior [22] on a road without VDRs. The proposed procedure allows estimating the increase in exhaust and FC emissions implied by the presence of RDVs on the road, being applicable to road sections containing any type of RDV from the average speed (VM) of a PVT to be evaluated. The success of the estimations increases with the consistency of the PVT associated with the evaluation scenario, since it has been shown that the estimation of pollutant emissions is relatively sensitive to the quality and accuracy with which the driving speed is described [23]. Therefore, an accurate and detailed knowledge of the actual speeds is necessary. In this sense, results obtained with different vehicles on different roads obtained significant increases in emission and FC rates in aggressive driving versus normal driving, showing that these parameters are influenced by the way of driving [24].

This manuscript is structured as follows: Section 2 describes resources and methods employed. Section 3 shows the experimentation carried out on track sections with trapezoidal section RDVs (RDV STA) and circular section RDVs (RDV SCP). Section 4 shows the analysis of the results on the chosen scenarios. Finally, Section 5 presents the conclusions, limitations and future work of the study.

## 2. - MATERIALS AND METHODS

### 2.1 CHARACTERIZATION

The method developed consists of: *i*) measuring the accelerations of a vehicle traveling through a VDR at a given speed; *ii*) calculating an average signal value representative of the measurements obtained in the Z-axis at that speed; *iii*) identifying critical events in the signal calculated from the acceleration amplitudes in that axis; *iv*) establishing indicators of the impact received by the vehicle when traveling through the VDR.

Accelerations in the XYZ system are obtained through the IMU of a smartphone using the Sense-it app while driving a vehicle over a section containing the RDV. The collected samples are dumped on a PC resulting in Excel spreadsheets. Subsequently, the field data are processed using Matlab®.

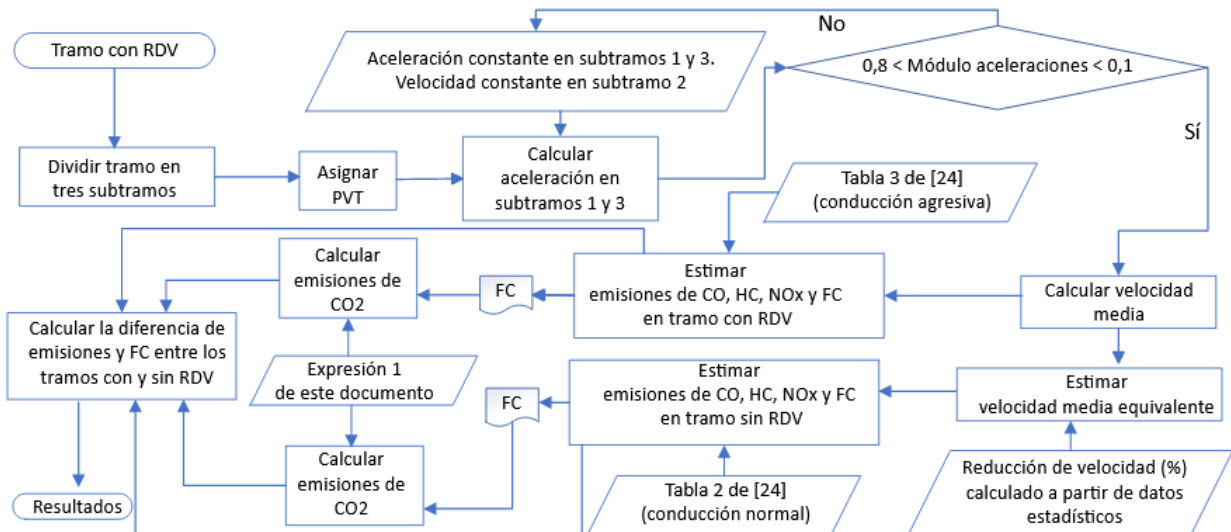
The processing stage eliminates unnecessary samples in the initial signals to the left and right of the evaluated RDV. The obtained signals are scaled to minimize the time lags between measurements corresponding to equal events and to obtain a coherent average value signal. Prior to scaling, the signals are normalized with the MinMax technique to compensate for amplitude and duration variations. Once scaled, their average value is calculated and filtered. To validate the processing, the correlation of the average value and of the signal resulting from filtering with the signal taken as a reference in the normalization process is analyzed.

In the acceleration curve are located the moments corresponding to the passage of the front (DR) and rear wheels (RT) through a change of gradient in the RDV. These are considered critical events because the vehicle receives an impact that significantly affects its motion in a direction perpendicular to the chassis. The transient response of the acceleration in the Z-axis of the accelerometer to a point impact is a damped oscillation whose trajectory can undergo modifications if, before reaching an equilibrium state, the vehicle experiences another impact. Therefore, test velocities, RDV dimensions, and the distance between RD and RT of the vehicle are used to identify critical points on the curve.

The characterization process ends by establishing the indicators of the impact caused by the RDV to the vehicle crossing it: *i*) subtraction between the maximum and minimum amplitude of the accelerations in the Z axis between two consecutive critical events ( $\Delta A_{MaxMin}$ ) and time elapsed between both amplitudes ( $T_{MaxMin}$ ); *ii*) maximum and minimum amplitude in absolute value recorded in the curve for that axis; *iii*) amplitude of the curve in that axis and time between maximum and minimum.

## 2.2 EXHAUST EMISSIONS AND FC

The developed method estimates the emissions of carbon monoxide (CO), carbon dioxide (CO<sub>2</sub>), total hydrocarbons (HC), nitrogen oxide (NO<sub>x</sub>) and FC in a section with RDVs versus the same without RDVs and calculates the difference between both estimates. Finally, the percentage increases are established as indicators of the environmental impact due to the presence of RDVs on the road. A schematic of the procedure is shown in Fig. 1.



Estimated increase in emissions and CF due to the presence of RDVs.

The method begins by assigning a PVT -to the section with RDV- composed of the initial and final speeds of each subsection into which it is divided. For this purpose, constant acceleration and deceleration are considered in the outbound and inbound subsections of the RDV, and constant speed in for the rest. Knowing these data -and the lengths of each sub-section- the value of the accelerations is calculated from the equations of uniformly accelerated motion. The resulting MV of the path is obtained using Merton's theorem. Based on the VM obtained in the section with RDVs, an equivalent mean velocity (EMV) is proposed as the estimated velocity higher than VM in the absence of RDVs. The percentage reduction of VM with respect to VME is estimated from statistical data of schemes with RDVs similar to those analyzed.

Exhaust emissions and FC are obtained from tabulated statistical data [24] for different speeds under normal and aggressive driving. On the one hand, the values obtained for CO, HC, NO<sub>x</sub> and FC at VM for aggressive driving are attributed to the section evaluated with RDV and those obtained at VME under normal driving are attributed to the section without RDV. This method requires that the absolute value of accelerations and decelerations in the section with RDV be between 0.85-1.10 m\*s<sup>-2</sup> - conditions of the measurement campaigns in [22]-[24] - and associates normal driving to the section without RDV. On the other hand, from the FC results, the theoretical CO emission rates<sub>2</sub> are obtained according to the expression (1) resulting from generalizing the stoichiometric relationship for gasoline combustion presented in [25] at different densities ( $\delta$ ).

$$\text{Emisiones de CO}_2 \left( \frac{\text{g}}{\text{km}} \right) = \text{FC} \left( \frac{\text{L}}{100 \text{ km}} \right) * 3,086 * \delta \left( \frac{\text{g}}{\text{L}} \right) \quad (1)$$

### 3. - EXPERIMENTATION

#### 3.1 MEASUREMENT OF PHYSICAL IMPACT

Acceleration measurements were taken with a smartphone (Samsung Galaxy S5) placed in a 1349 cm<sup>3</sup> Mazda 2 while driving on two sections with STA and SCP type RDVs. During the tests, the smartphone was held stationary in a horizontal position while the co-driver took the measurements (Fig. B, supplementary material).

For the RDV STA, ten measurements at 30 and ten at 10 km/h were performed. For the RDV SCP, ten at 30 and ten at 20 km/h. A time series with a sampling frequency equal to 100 Hz was obtained from each measurement. For each set of ten measurements the average value was obtained and a median filter was applied.

To apply the MinMax method to each set of measurements, the signal whose difference in amplitudes between maximum and minimum was greater was taken as a reference. In order to choose the most appropriate correlation analysis technique, the linear trend of the variables and the normality of the distribution of their data were checked.

In all cases the scatter diagrams of the average values versus the reference signals showed a linear trend, but none of the variables presented a normal distribution of data due to the presence of extreme values in the area corresponding to the passage through the RDVs. Therefore, the most representative average values were validated from Spearman's correlation coefficient ( $\rho$ ), recommended when the data present extreme values or non-normal distributions [26].

From the correlation analysis between the most representative average value and reference signal -for each test speed- resulted: *i*)  $\rho$  coefficient values of 0.4603 at 30 km/h and 0.3303 at 10 km/h for the RDV STA; *ii*)  $\rho$  coefficient values of 0.4239 at 30 km/h and 0.3925 at 20 km/h for the RDV SCP; and *iii*) probabilistic values equal to 0.000 in all cases.

All the  $\rho$  coefficients were different from zero and the p-values were less than the significance level (0.05), indicating in all cases the rejection of the null hypothesis that there was no correlation. Therefore, the alternative hypothesis that there was a statistically significant correlation between the signals analyzed was accepted.

##### 3.1.1 RDV STA

This section evaluates a trapezoidal cross-section VDR for a raised pedestrian walkway with asphalt ramps and cobblestone plateau located in Avenida Reyes Católicos, located in Inca (Mallorca). Fig. C (included in supplementary material) shows the section containing the evaluated RDV (R2), a photo and its dimensioned section.

The path profile has four changes of gradient: entry into ramp 1 (ER1), exit from ramp 1 (SR1), entry into ramp 2 (ER2) and exit from ramp 2 (SR2). This results in eight critical events (shown in Fig. 2), four corresponding to the passage of the vehicle DRs and four to the passage of the RTs. To quantify the physical impact of the RDV on the vehicle, expression (2) is used, obtaining values between -2,817 N and 3,073 N.

$$\vec{F} = m(a_z - 9,8 * \cos \alpha) \quad (2)$$

where  $m$  is the total mass of vehicle and passengers,  $a_z$  the acceleration obtained in the Z-axis,  $\alpha$  the inclination of the ramp, and  $\vec{F}$  the force in the Z-axis due to the impact.

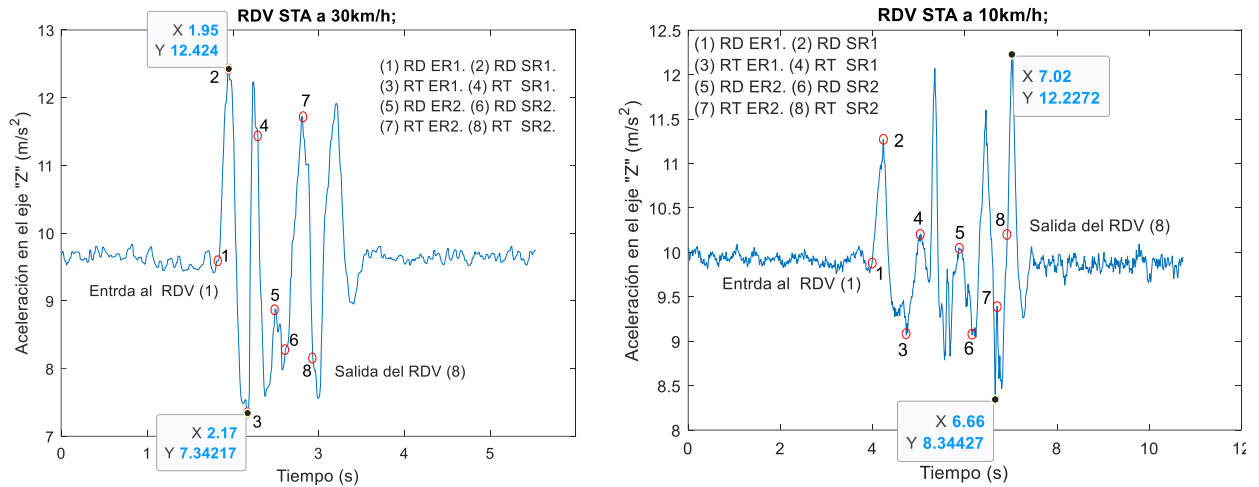


Fig. 2. Average value signals representative of the experimentation with the RDV STA.

### 3.1.2 RDV SCP

A rubber and elastomers prefabricated circular cross-section RDV located in Puig de Massanella Street, located in Inca (Mallorca) is evaluated. Fig. D (included in supplementary material) shows the scenario of the evaluated RDV (R1), a photo and its dimensioned section.

The path profile presents two changes of gradient: entrance to the VDR (ER1) and exit from the VDR (SR1). This gives rise to four critical events (shown in Fig. 3), two corresponding to the passage of the RDV of the vehicle and two to the passage of the RT. To quantify the physical impact of the RDV on the vehicle, the expression (2) - considering  $\alpha$  the inclination of the RDV- obtaining values between -3,100 N and 5,405 N is used.

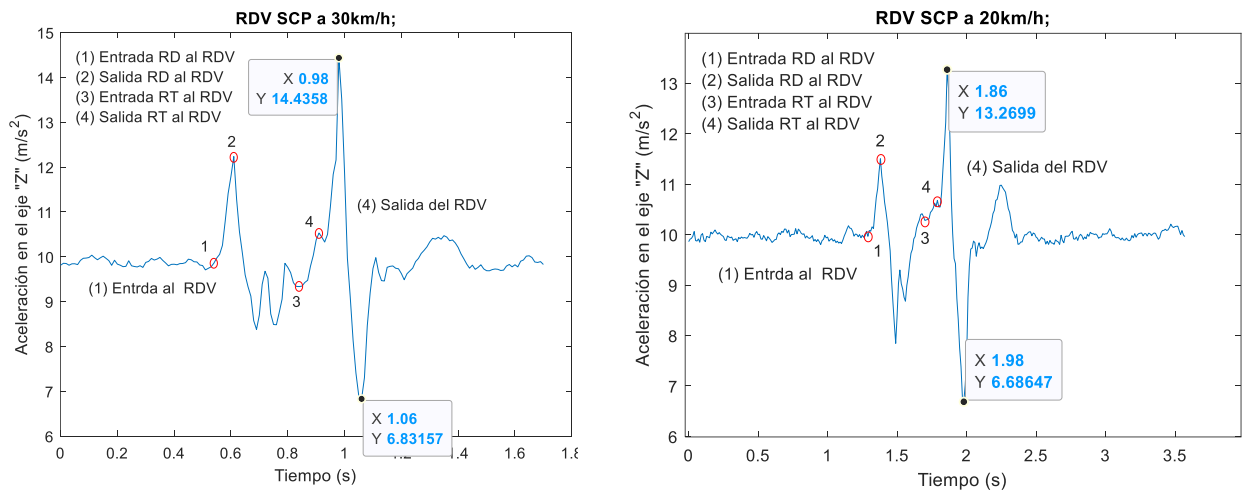


Fig. 3. Average value signals representative of the RDV SCP experimentation.

## 3.2 INFERENCE OF EXHAUST EMISSIONS AND FUEL CONSUMPTION

The inference method is applied to a three-way catalytic converter (TWC) gasoline passenger car with 1.4 L capacity driving on the sections containing the characterized RDVs. The speed is limited to 30 km/h in both scenarios.

### 3.2.1 Section with RDV STA

The PVT is defined by the initial and final velocities of each subsection (expression 3). Fig. E (included in supplementary material) shows the lengths of the evaluated section (i.e., exit from R1 to exit from R2) and a plot of the PVT.

$$PVT = \{V1, V2, V3, V4, V5\} = \{11, 25, 25, 11, 11\} \left(\frac{\text{km}}{\text{h}}\right) \quad (3)$$

The calculated MV for the RDV path is 18.75 km/h and the acceleration values obtained in sub-sections 1 and 3 (i.e., 0.97 m\*s<sup>-2</sup> and -0.97 m\*s<sup>-2</sup>, respectively) are within the range of application of the method. Therefore, the HC, NO<sub>x</sub> and FC emissions attributed to the section with RDV have been obtained by extrapolating the MV in Table 3 of [24] with the Spline method. CO emissions have been obtained by interpolating the MV in the graph corresponding to car7 in Fig. 2 of [24].

Considering the similarity observed between scheme A of [2] and the configuration of the section with VDR, the magnitude of VME is estimated taking Table 5 of [2] as a reference. Under these conditions, it is calculated that the speed reduction that a medium vehicle would experience (Table 10 of [2]) when passing through a road with RDV versus passing without RDV is 29.50 %, so the VME estimate is 26.60 km/h. The CO, HC, NO<sub>x</sub> and FC emissions attributed to the section without RDV have been obtained by interpolating the VME in Table 2 of [24] with the Spline method. CO<sub>2</sub> emissions have been obtained in both cases from FC according to expression (1) considering 95 octane unleaded gasoline of density  $\delta = 750$  g/L.

### 3.2.2 Section with VDR SCP

The PVT (4) is defined as in 3.2.1. Fig. F (included in supplementary material) shows the lengths of the evaluated section (i.e., output of R2 to output of R1) and a plot of the PVT.

$$PVT = \{V1, V2, V3, V4, V5\} = \{20, 30, 30, 20, 20\} \left(\frac{\text{km}}{\text{h}}\right) \quad (4)$$

The MV calculated for the RDV path is 27.58 km/h. The accelerations in subsections 1 and 3 (i.e., 0.96 m\*s<sup>-2</sup> and -0.96 m\*s<sup>-2</sup> respectively) allow the application of the method. Taking as a reference the experimentation of [5] with RDVs with the same characteristics as those of this study, a speed reduction of 13.5% has been inferred in the section with RDV and the VME has been estimated at 31.99 km/h. Emissions and FC are obtained, in this case always interpolating, following the same procedure as in 3.2.1. Emissions and FC are obtained, in this case always interpolating, following the same procedure as in 3.2.1.

## 4.- RESULTS

The identification of critical events in the representative average value signals has made it possible to establish indicators of the physical impact experienced by the vehicle when driving on the RDVs according to Tables 1 and 3. In addition, the resulting emission and FC values are shown in Tables 2 and 4.

### 4.1 RDV STA

Section of the RDV	$\Delta A_{\text{MaxMin}} \text{ (m/s}^2\text{)}$		Distance (m)	$T_{\text{MaxMin}} \text{ (s)}$	
	30 Km/h	10 Km/h		30	10
RD pass through ER1 to RD pass through SR1	2,83	1,38	1	0,11	0,24
Passing RD through SR1 to passing RT through ER1	5,078	2,2	1,54	0,23	0,50
RT pass through ER1 to RT pass through SR1	4,89	1,14	1	0,06	0,31
RT pass through SR1 to RD pass through ER2	3,84	3,281	1,66	0,08	0,83
Passing RD through ER2 to passing RD through SR2	0,89	0,98	1	0,08	0,29
Passage of RD through SR2 to passage of RT through	3,44	3,26	1,54	0,19	0,20
RT pass through ER2 to RT pass through SR2	3,57	1,73	1	0,19	0,22
RT passing through SR2 to equilibrium state	4,35	2,97	4,61   1,04	0,21	0,24
<b>Maximum, absolute minimum and amplitude of the acceleration curve (m/s<sup>2</sup>) at 30 Km/h</b>					
Max. (passage of RD through SR1) = 12.42	Min. value (RT pass through ER1) =		5.078 (time between peaks = 0.23 s)		
<b>Maximum, absolute minimum and amplitude of the acceleration curve (m/s<sup>2</sup>) at 10 Km/h</b>					
Max. (0.10 s after RDV output) = 12.23	Min. (0.36 s prior to RDV output) = 8.34		3,886 (time between peaks = 0,36 s)		

Table 1. Indicators of the impact caused by the RDV STA at 30 and 10 km/h.

		Section with VDR (1)	Section without VDR (2)	Emissions increase [(1) - (2)] (%)
<b>Broadcast</b> (g*km <sup>-1</sup> )	CO	35,34	3,055	1.057
	HC	1,157	0,239	384
	NOx	0,290	0,169	
	CO <sub>2</sub>	413,60	262,23	58
FC (L/100km)		17,87	11,33	58

Table 2. Emissions and FC results for RDV STA of the studied tourism.

The amplitude of the acceleration curve at 30 km/h is 30.67% higher than at 10 and its  $T_{MaxMin}$  is 36.11% lower at 30 km/h than at 10. In 87.5% of the events result in higher  $\Delta A_{MaxMin}$  at lower  $T_{MaxMin}$  at 30 km/h than at 10. The highest  $\Delta A_{MaxMin}$  at 30 km/h is 54.77% higher than the highest at 10 and  $T_{MaxMin}$  is 72.29% lower at 30 km/h than at 10.

#### 4.2 RDV SCP

Section of the RDV	$\Delta A_{MaxMin}$ (m/s <sup>2</sup> )		Distance (m)	$T_{MaxMin}$ (s)	
	30 Km/h	20 Km/h		30 Km/h	20 Km/h
RD input to RDV to RD output from RDV	2,38	1,525	0,60	0,07	0,11
RD output from RDV to RT input to RDV	3,93	3,65	1,94	0,08	0,11
RT input to the RDV to RT output from the RDV	1,194	0,40	0,60	0,07	0,09
RT output from RDV to steady state	7,61	6,584	1,91   3,41	0,08	0,12
<b>Maximum, absolute minimum and amplitude of the acceleration curve (m/s<sup>2</sup>) at 30 Km/h</b>					
Max. (0.01 s after RDV output) = 14.44		Min. (0.0 s after RDV output) = 6.832		7.61 (time between peaks = 0.08 s)	
<b>Maximum, absolute minimum and amplitude of the acceleration curve (m/s<sup>2</sup>) at 20 Km/h</b>					
Max. (0.07 s after RDV output) = 13.27		Min. (0.19 s after RDV output) = 6.68		6,584 (time between peaks = 0,12 s)	

Table 3. Indicators of the impact caused by the RDV SCP at 30 and 20 Km/h

		Section with VDR (1)	Section without VDR (2)	Emissions increase [(1) - (2)] (%)
<b>Broadcast</b> (g*km <sup>-1</sup> )	CO	26,68	2,87	829,62
	HC	1,137	0,234	385,90
	NOx	0.271	0,155	74,84
	CO <sub>2</sub>	354,81	240,24	47,69
FC (L/100km)		15,33	10,37	47,83

Table 4. Emissions and CF results for the tourism studied.

The amplitude of the acceleration curve at 30 km/h is 15.58% higher than at 20 and its  $T_{MaxMin}$  is 33.33% lower at 30 km/h than at 20. In 87.5% of the events result in higher  $\Delta A_{MaxMin}$  at lower  $T_{MaxMin}$  at 30 km/h than at 20. The highest  $\Delta A_{MaxMin}$  at 30 km/h is 7.12% higher than the highest at 20 and  $T_{MaxMin}$  is 27.27% lower at 30 km/h than at 20.

## 5.- CONCLUSIONS

The presence of speed humps in traffic calming measures induces abrupt speed changes involving higher vehicle emissions and FC. To analyze their impact, this work presented a procedure based on two methods applied to RDVs. The first one measures the physical impact on a vehicle from acceleration data taken with a smartphone app. The second one infers its impact on pollution according to the PVT of a journey.

On the one hand, the analysis carried out indicated that: *i)* vehicle displacement in the direction perpendicular to the chassis increases when driving through a VDR; *ii)* the impact is greater at higher speeds and is influenced by the vehicle's wheelbase, angle of attack and wheelbase. Considering a standard vehicle with two passengers, it was determined a force between -2,817 N and 3,073 N when passing through an RDV STA and between -3,100 N and 5,405 N in an RDV SCP. On the other hand, the developed method found

an increase of 1,057 % CO, 384 % HC, 72 % NO<sub>x</sub>, 58 % CO<sub>2</sub> and 58 % FC emissions when reducing the speed of a vehicle from 30 to 10 km/h in a RDV STA. Similarly, reducing the speed from 30 to 20 km/h in a SCP RDV implied 829.62 % increase in CO emissions, 385.90 % HC, 74.84 % NO<sub>x</sub>, 47.69 % CO<sub>2</sub> and 47.83 % FC.

This work suggests that increasing the length of ramps by optimizing the wheelbase to grade ratio - in future RDV designs - would reduce the impact they cause.

The measurements made with this method, which employs an app integrated into a citizen science web platform, form an important data set that can be extended to multiple scenarios bringing environmental sensitivity and ongoing knowledge to the state of the art. The methodology is limited to the availability of statistical data that meet the requirements to be implemented. On the other hand, it estimates an EMV corresponding to the section without RDVs different from the MV corresponding to the sections with RDVs and does not implement a procedure that validates the results of emissions and CF. Nevertheless, the results obtained serve as a reference for practical purposes.

Future work is aimed at reducing the negative consequences of traffic in urban areas by implementing traffic calming measures that do not involve abrupt speed reductions. Intelligent safety systems based on I2V (infrastructure-to-vehicle) or P2V (pedestrian-to-vehicle) communication that warn in advance of the risk of being run over could be an ecological alternative at crosswalks since they would eliminate the need to reduce speed in the absence of a condition, which does not occur when there is a permanent presence of RDVs. It is also proposed to extend the study to other types of VDRs, considering particle emissions due to brake pad abrasion and tire wear, as well as to investigate mathematical models that describe the environmental repercussion of the physical impact they cause on the vehicle.

## REFERENCES

- [1] S. Hallmark, K. Knapp, G. Thomas, and D. Smith, "Temporary Speed Hump Impact Evaluation", CTRE Project 00-73, pp. 158, 2002.
- [2] P. G. Boulter, J. M. Hickman-Davis, S. Latham, P. Davison, and P. Whiteman, "The impacts of traffic calming measures on vehicle exhaust emissions", *Transport Research Laboratory*, TRL REPORT 482, pp. 96, 2001.
- [3] A. Vaitkus *et al.*, "Traffic Calming Measures: An Evaluation of the Effect on Driving Speed", *PROMET - Traffic&Transportation*, vol. 29, no. 3, pp. 275-285, 2017. DOI: <http://dx.doi.org/10.7307/ptt.v29i3.2265>
- [4] BOE.es - BOE-A-2008-17255 Orden FOM/3053/2008, de 23 de septiembre, por la que se aprueba la Instrucción Técnica para la instalación de reductores de velocidad y bandas transversales de alerta en carreteras de la Red de Carreteras del Estado.
- [5] M. Pau and S. Angius, "Do speed bumps really decrease traffic speed? An Italian experience," *Accid. Anal. Prev.*, vol. 33, no. 5, pp. 585-597, 2001. DOI: [https://doi.org/10.1016/S0001-4575\(00\)00070-1](https://doi.org/10.1016/S0001-4575(00)00070-1)
- [6] G. Watts, "Road humps for the control of vehicle speeds," *Transp. Road Res. Lab. Dep. Environ.* TRRL. Rep. LR 597, pp. 44, 1973.
- [7] R. Leboeuf, S. Seriani and A. Jané. "Impacto de resaltos reductores de velocidad en automóviles y sus ocupantes", Conference Paper, pp.1-16, 2014. DOI: <http://dx.doi.org/10.13140/2.1.3285.3448>
- [8] D. G. Pozuelo, A. Gauchia, E. Olmeda, and V. Diaz, "Bump Modeling and Vehicle Vertical Dynamics Prediction", *Hindawi Publishing Corporation Advances in Mechanical Engineering*, vol. 2014, Article ID 736576, pp.1-10. DOI: <http://dx.doi.org/10.1155/2014/736576>
- [9] Q. Mourcou, A. Fleury, C. Franco *et al.*, "Performance Evaluation of Smartphone Inertial Sensors Measurement for Range of Motion", *Sensors*, pp. 1-20, 2015. DOI: <http://dx.doi.org/10.3390/s150923168>
- [10] V. Gikas and H. Perakis, "Rigorous performance evaluation of smartphone GNSS/IMU sensors for ITS applications", *Sensors*, pp. 1-21, 2016. DOI: <http://dx.doi.org/10.3390/s16081240>
- [11] A. Mukherjee & S. Majhi, "Characterisation of road bumps using smartphones", *European Transport Research Review*, *Springer*, pp. 1-12, 2016. DOI: <http://dx.doi.org/10.1007/s12544-016-0200-1>
- [12] M. Sharples, M. Aristidou, E. Villasclaras, "The Sense-it App: A Smartphone Sensor Toolkit for Citizen Inquiry Learning", *International Journal of Mobile and Blended Learning*, vol. 9, no. 2, pp. 1-16, 2017. DOI: <http://dx.doi.org/10.4018/IJMBL.2017040102>
- [13] NICE, "Resource impact report: Air pollution: outdoor air quality and health", *NICE guideline*, pp. 1-63 n<sup>o</sup>, 2017.
- [14] P. Baltrėnas, T. Januševičius, and A. Chlebnikovas, "Research into the impact of speed bumps on particulate matter air pollution", *Meas. J. Int. Meas. Confed.*, vol. 100, pp. 62-67, 2017. DOI: <https://doi.org/10.1016/j.measurement.2016.12.042>
- [15] N. Haworth and M. Symmons, "The Relationship Between Fuel Economy and Safety Outcomes", no. 188, p. 57, 2001, Accessed: Jun. 14, 2021. 280 [Online]. Available: <https://trid.trb.org/view/732971>
- [16] L. Int Panis, S. Broekx, and R. Liu, "Modelling instantaneous traffic emission and the influence of traffic speed limits", *Sci. Total Environ.*, vol. 371, no. 1-3, 282 pp. 270-285, 2006. DOI: <https://doi.org/10.1016/j.scitotenv.2006.08.017>
- [17] K. Ayyildiz, F. Cavallaro, S. Nocera, and R. Willenbrock, "Reducing fuel consumption and carbon emissions through eco-drive training", *Transp. Res. Part 284 F Traffic Psychol. Behav.*, vol. 46, pp. 96-110, 2017. DOI: <https://doi.org/10.1016/j.trf.2017.01.006>
- [18] J. Q. Hansen, M. Winther, and S. C. Sorenson, "The influence of driving patterns on petrol passenger car emissions", *Sci. Total Environ.*, vol. 169, no. 1-3, pp. 129-139, 1995. DOI: [https://doi.org/10.1016/0048-9697\(95\)04641-D](https://doi.org/10.1016/0048-9697(95)04641-D)
- [19] Daham, B., Andrews, G., Li, H., Partridge, M. *et al.*, "Quantifying the Effects of Traffic Calming on Emissions Using On-road Measurements," *SAE Technical Paper 2005-01-1620*, pp. 1-17, 2005. DOI: <https://doi.org/10.4271/2005-01-1620>

- [20] C. Graham Heeks, "Deformable speed bump", Patent Application Publication. US 2002/0085881 A1, 2002.
- [21] J. M. L. Domínguez, F. Al-Tam, T. de J. M. Sanguino, and N. Correia, "Analysis of machine learning techniques applied to sensory detection of vehicles in intelligent crosswalks" *Sensors*, vol. 20, no. 21, pp. 1-19, 2020. DOI: <http://dx.doi.org/10.3390/s20216019>
- [22] I. De Vlieger, "On-board emission and fuel consumption measurement campaign on petrol-driven passenger cars", *Atmos. Environ.*, vol. 31, no. 22, pp. 3753-3761, 1997, DOI: [https://doi.org/10.1016/S1352-2310\(97\)00212-4](https://doi.org/10.1016/S1352-2310(97)00212-4)
- [23] M. André and U. Hammarström, "Driving speeds in Europe for pollutant emissions estimation", *Transp. Res. Part D Transp. Environ.*, vol. 5, no. 5, pp. 321-335, 2000. DOI: [https://doi.org/10.1016/S1361-9209\(00\)00002-X](https://doi.org/10.1016/S1361-9209(00)00002-X)
- [24] I. De Vlieger, D. De Keukeleere, and J. G. Kretzschmar, "Environmental effects of driving behaviour and congestion related to passenger cars", *Atmos. Environ.*, vol. 34, no. 27, pp. 4649-4655, 2000. DOI: [https://doi.org/10.1016/S1352-2310\(00\)00217-X](https://doi.org/10.1016/S1352-2310(00)00217-X)
- [25] M. T. Oliver-Hoyo and G. Pinto, "Using the relationship between vehicle fuel consumption and CO2 emissions to illustrate chemical principles", *Journal of Chemical Education*, vol. 85, no. 2, pp. 218-220, 2008. DOI: <http://dx.doi.org/10.1021/ed085p218>
- [26] P. Fernández S. and S. Pértega Díaz, "Investigación: relación entre variables cuantitativas", Unidad de Epidemiología Clínica y Bioestadística. Complejo Hospitalario Juan Canalejo. A Coruña.

## SUPPLEMENTARY MATERIAL

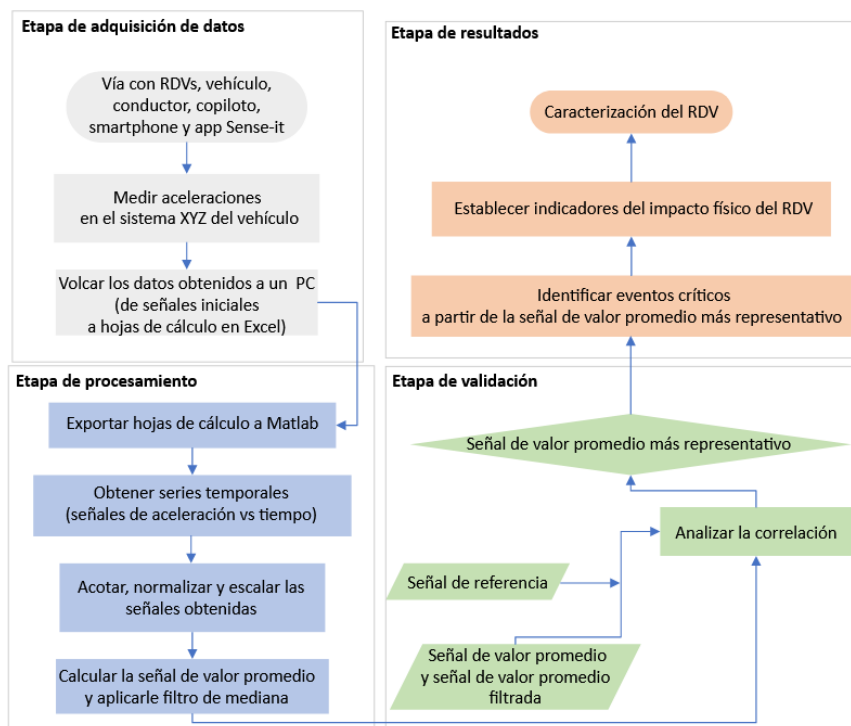


Fig. A. Diagram of stages of the characterization method.



Fig. B. Location of the smartphone in the vehicle and acceleration graph in the X, Y, Z axes vs. time.

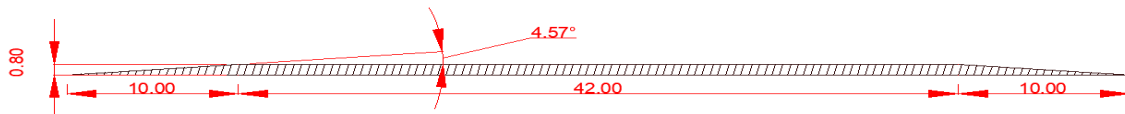


Fig. C. Top image: track section with evaluated VDR STA. Source: image obtained from IDEIB (Spatial Data Infrastructure of the Balearic Islands) and edited by the authors. Bottom image: longitudinal section of the RDV STA.



Fig. D. Top image: track section with evaluated RDV SCP. Source: image obtained from IDEIB (Spatial Data Infrastructure of the Balearic Islands) and edited by the authors. Bottom image: longitudinal section drawing of the RDV SCP.

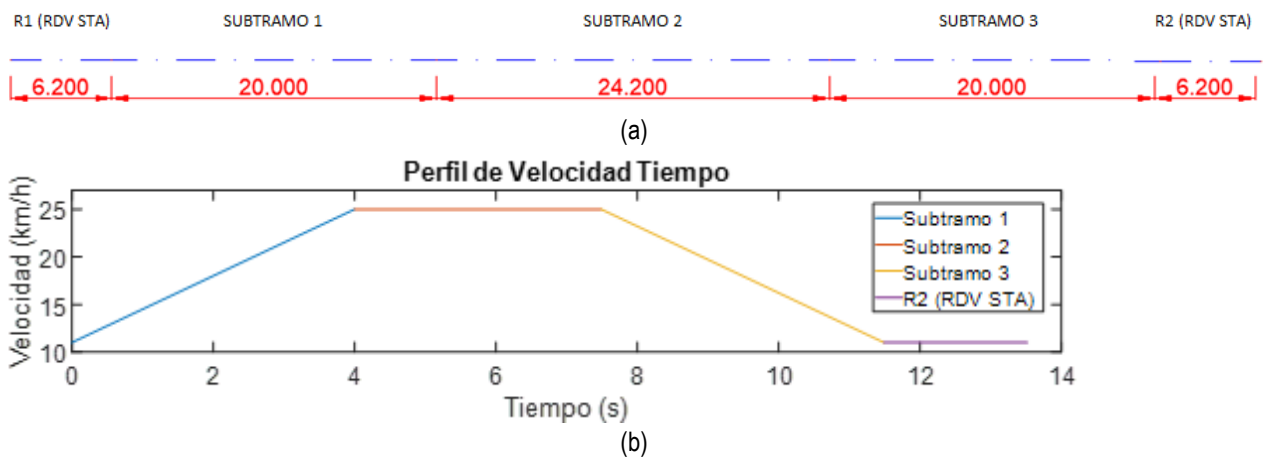
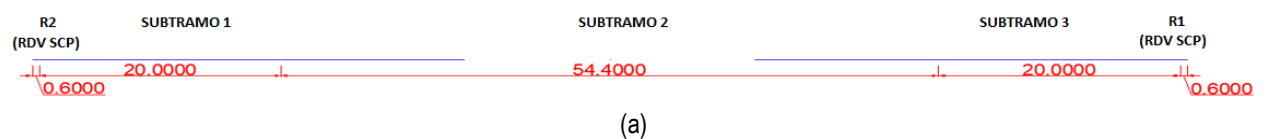


Fig. E. Lengths in meters of the studied section (a) and speed vs. time profile of the section with RDV STA (b).



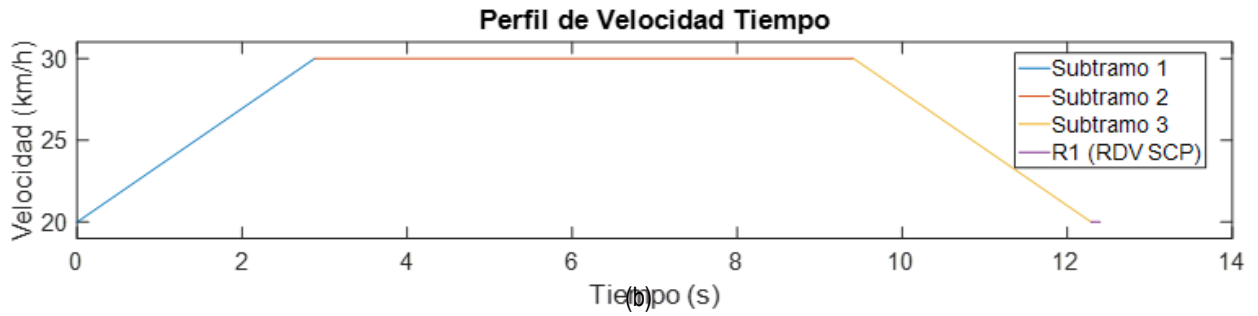


Fig. F. Lengths in meters of the section studied (a) and speed vs. time profile of the section with RDV SCP (b).